International Journal of Mathematical Archive-4(12), 2013, 116-126
Available online through www.ijma.info ISSN 2229 – 5046

ELECTROHYDRODYNAMIC RAYLEIGH-TAYLOR INSTABILITY IN A NON-NEWTONIAN FLUID

Krishna B. Chavaraddi*
Department of Mathematics, Government First Grade College, Yellapur (U.K)-581 359, Karnataka.

(Received on: 28-11-13; Revised & Accepted on: 31-12-13)

ABSTRACT

With the growing importance of non-Newtonian fluids in modern technology and industries, investigations on such fluids are desirable. In the present paper is to study the Rayleigh-Taylor instability (RTI) in a thin layer of an incompressible non-Newtonian fluid, assuming it obeys power law, confined above by a interface with a heavier fluid, and below by an impermeable rigid boundary subject to linear stability analysis. The formulation developed in the present work is to evaluate the influence of the effects of non-Newtonian fluid, surface tension and the layer thickness on the RTI using the approximations described by Rudraiah et al., (1996). These approximations simplify the power-law equation and pave the way to find analytical solution for velocity distribution which will be used in the dispersion relation obtained using suitable boundary and interface conditions.

Key words: *Rayleigh-Taylor instability (RTI), Power-law fluid, no shear condition, electric field.*

1. INTRODUCTION

Though this topic encompasses different areas, such as space science, astrophysics and so on, its application is found mainly in solidification processes, inertial fusion energy (IFE) and cooling of machineries. So it is imperative that the present processing techniques and systems have to be modified to improve the quality of the final product. One of the most demanding engineering issues in IFE reactors is the design of a reaction chamber that can withstand the intense photons, neutrons and charged particles due to the fusion event. Rapid pulsed deposition of energy within thin surface layers of the fusion reactor components such as the first wall may cause severe surface erosion due to ablation. An innovative concept for the protection of IFE reactor cavity first walls from the direct energy deposition associated with soft X-rays and target debris is the thin liquid film protection scheme. In this concept, a thin film of molten liquid lead is fed through a silicon carbide first wall to protect it from the incident irradiations. In IFE, the hallow shells are filled with an equal mixture of Deuterium and Tritium (DT) fluid at high pressure and then solidified to the cryogenic temperature so that the DT-fluid freezes forming a thin mushy coating on the inside of the ablative surface of the shell wall. The direct– drive laser heat at this ablative surface directly causing surface instabilities.

The following different types of interfacial or surface instabilities are encountered:
(i) Rayleigh-Taylor instability (RTI)
(ii) Kelvin-Helmholtz Instability(KHI)
(iii) Richtmyer-Meshkov Instability(RMI)

As discussed above the surface instabilities at target surface, there has been a considerable practical interest in the study of surface instability of the Rayleigh-Taylor type. The RTI occurs at an interface between a dense fluids supported by a less dense fluid when the latter is at high pressure. These instabilities have attracted considerable interest both theoretically(see Chandrasekhar, 1961 and Sharp, 1984) and experimentally (see Kull, 1991) because of the importance in understanding the control and exploitation of many of the basic physical, chemical and biological processes. Babchin *et al.*, (1983) have studied the non-linear RT instability in a thin Newtonian fluid film when the wavelength is much greater than the film thickness. Later, Brown (1989) relaxed this assumption on the wavelength and studied the RT instability in a finite thin layer of a viscous fluid using the combined Stokes and lubrication approximations as Babchin *et al.*, (1983). Recently, Rudraiah *et al.*, (1997, 1996) have extended the work of Brown (1989) to include the viscosity stratification and the effect of oblique magnetic field in Newtonian fluids. The works mentioned above are mainly concerned with Newtonian fluid. However, there is a rather different subject area of polymer processing applications, where, the polymers having chain molecules and behaving as a viscoelastic fluid over longer times have a range of unlikely behavior. In conditions of shear flow, they develop instabilities that of linked polymers. This failure has been shown to occur by the formation and growth of planar defects called crazes. When this crazing is accelerated by the presence of plasticizing fluid, it is likely that a thin layer of material adjacent to the heavy fluid will plasticize undergoing RTI as in the Newtonian fluid discussed by Brown (1989).

Corresponding author: Krishna B. Chavaraddi, E-mail: ckrishna2002@yahoo.com*
Department of Mathematics, Government First Grade College, Yellapur(U.K)-581 359, Karnataka.

The surface instabilities play a significant role is the synovial joints which are freely movable joints. They consist of an articulate cartilage which is a two–phase deformable porous material having fixed electrical charges embedded in the tissue and a positively charged liquid (see Rudraiah *et al*., 1998, Ng *et al*., 2005) and the synovial fluid which is in general a non-Newtonian fluid having viscosity 1000 times that of water. One of the causes for degenerative changes in cartilages, evolving through osteoarthritis due to old age, Traumatic arthritis due to injuries, Rheumatoid arthritis due to diseases, is due to surface instabilities of the type RTI occurring at the interface between artificial cartilage and synovial fluid. Since the cartilage is a fluid saturated porous medium layer the synovial fluid, there is a need to understand the nature of surface instability at the cartilage lined with the non-Newtonian nature of synovial fluid for the effective design of artificial joints.

A great deal of research on RTI has been carried out in a Newtonian fluid. But, very little is known about RTI in a non-Newtonian fluid with application to polymer processing. As stated earlier, one of the objectives in studying the RTI in a non-Newtonian fluid has been to develop an understanding of the responses of the complex systems to various types of deformation, so that useful information is generated for practical purposes. The literature on RTI reveals that the mathematical modeling of non-Newtonian fluid is very complicated and beyond the comprehension of obtaining exact solution, the experimental works in RTI pertain to simplified flow systems and situations which are too ideal and have little importance in actual practice. Therefore, with an interest for practical application, it is desirable to compromise complicated mathematical models and the pure estimates of simple experimental results leading to thumb rule formula.

The study of RT instability in non-Newtonian fluids in a finite thickness layer obeying power law viscoelastic fluid model is of considerable interest in material processing, particularly, in understanding the defects in the manufacture of new type of polymer materials used in many industrial applications. These defects are bound to occur at very low flow rates in materials having very high viscosity. The control of viscosity can be achieved with increasing rate of shear in a steady shear flow. The understanding and control of non-Newtonian power law fluid (pseudoplastic or dilatant), provides, from the technical point of view, useful information in materials processing. Recently, Rudraiah *et al.,* (2000) have studied the RTI in a finite thickness layer of a non-Newtonian fluid and they concluded that the nature of the dispersion curve is influenced by both the reciprocal of the characteristic length and the non-Newtonian parameter, with the film thickness just affecting the nature of the growth rate of instability, in the sense that an increase in film thickness increases the growth rate. Not much work has been done in non-Newtonian fluid. Also, Rudraiah et al., (2011) have investigated the Electrohydrodynamic RTI in a non-Newtonian fluid layer bounded above by a porous layer. To achieve this objective, this paper is planned as follows. The basic equations for poorly conducting non-Newtonian power law fluid in the presence of electric field are given in section 2 with suitable approximations and boundary conditions. The dispersion relation of RTI in the presence of electric field using boundary and surface conditions is derived in section 3. The importance conclusions are drawn in the final section.

2. MATHEMATICAL FORMULATION

The physical configuration is shown in Fig.1. It consists of a thin target shell in the form of a thin film of unperturbed thickness *h* (region 1) filled with an incompressible, viscous, poorly electrically conducting non-Newtonian lighter power-law fluid of density ρ_l bounded below by a rigid surface at *y=0* and above by an incompressible, viscous poorly conducting non-Newtonian heavier power-law fluid of density ρ_p of large extent compared to the shell thickness *h*. Also, the electrodes are embedded at the rigid surface *y* = 0 as well as at the interface *y* = *h* and there by an electric field is generated in fluid-power law fluid composite system. The fluid in the thin film is set in motion by acceleration normal to the interface whereas in the region-2 it is assumed to be static and small perturbations are amplified when acceleration is directed from the lighter fluid in the thin film to the heavier fluid. The instability at the interface in the presence of electric field is known as

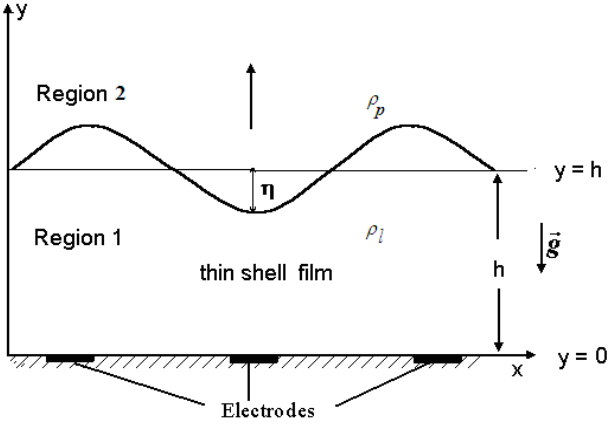

Fig.1: Physical Configuration

electrohydrodynamic Rayleigh-Taylor instability (ERTI). To investigate this ERTI, we consider a rectangular coordinate system (*x, y*) with the x-axis parallel to the film and y-axis normal to it. The interface between the power law fluid and thin film (fluid) is described by $\eta(x,t)$.

The basic equations for poorly electrically conducting non-Newtonian fluid in the thin film considered here are (see Rudraiah and Kaloni, 1990):

The conservation of mass:

$$\nabla \cdot \vec{q} = 0 \tag{2.1}$$

The conservation of momentum:

$$\rho \frac{D\vec{q}}{Dt} = -\nabla p + \nabla \cdot \vec{\tau} + \rho_e \vec{E} \tag{2.2}$$

The conservation of electric charges:

$$\frac{\partial \rho_e}{\partial t} + \left(\vec{q} \cdot \nabla\right)\rho_e + \nabla \cdot \vec{J} = 0 \tag{2.3}$$

The Maxwell's equations:

$$\nabla \cdot \vec{E} = \frac{\rho_e}{\varepsilon_e} \tag{2.4a}$$

$$\nabla \times \vec{E} = 0 \quad \text{or} \quad \vec{E} = -\nabla \varphi \tag{2.4b}$$

$$\vec{J} = \sigma \vec{E} \tag{2.4c}$$

$$\sigma = \sigma_0 \left[1 + \alpha_h (C - C_0)\right]. \tag{2.4d}$$

The physical quantities appearing in the above equations are defined in the nomenclature.

The stress tensor $\vec{\tau}_i$ expressed as

$$\vec{\tau}_i = k_1 \left\{ \left| \frac{1}{2}\left(\frac{1}{2}\dot{\gamma}_i : \dot{\gamma}_i \right)^{\frac{m-1}{2}} \right| \right\} \dot{\gamma}. \tag{2.5}$$

here k_1 is the consistency index and $\dot{\gamma}$ is the rate of strain given by

$$\dot{\gamma}_{i,j} = \left(\frac{\partial q_i}{\partial x_j} + \frac{\partial q_j}{\partial x_i} \right) \dot{\gamma}. \tag{2.6}$$

The electrical conductivity σ varies with concentration C of deuterium-tritium as in Eq. (2.3). Then assuming negligible advection of concentration, we have

$$\frac{d^2 C}{dy^2} = 0 \tag{2.7}$$

with

$$C = C_0 \quad \text{at} \quad y = 0 \tag{2.8a}$$

$$C = C_1 \quad \text{at} \quad y = h. \tag{2.8b}$$

Solving Eq. (2.7) using the given conditions and substituting this solution in Eq. (2.4d), we get

$$\sigma = \sigma_0 \left[1 + \alpha y\right] \approx \sigma_0 e^{\alpha y} \tag{2.9}$$

where $\alpha = \alpha_h \Delta C / h$ and $\Delta C = C_1 - C_0$. We assume the frequency of charge distribution is smaller than the corresponding relaxation frequency of the electric field, and hence the time derivative of ρ_e is negligible compared to $\nabla \cdot (\sigma E)$ in Eq. (2.3). From this, we get

$$\frac{\partial^2 \phi}{\partial x^2} + \frac{\partial^2 \phi}{\partial y^2} + \alpha \frac{\partial \phi}{\partial y} = 0 . \tag{2.10}$$

The above equation has to be solved subject to the boundary conditions

$$\phi = \frac{v_0 x}{h} \quad at \quad y = 0 \tag{2.11}$$

$$\phi = v_0 \frac{(x - x_0)}{h} \quad at \quad y = h \tag{2.12}$$

These conditions arise due to embedded electrodes at $y = 0$ and $y = h$ and permits a linear variation of ϕ with x.

2.1 Assumptions and approximations

To investigate the problem posed in this paper, following Rudraiah *et. al.*, (1996), we make use of the following electrohydrodynamic approximations:

(i) The film thickness h is much smaller than the thickness H of the porous layer bounded above the film. That is,
$h << H$.

(ii) The Strouhal number S is assumed to be negligibly small.

$$S = \frac{L}{T U} << 1$$

The physical quantities are defined in the nomenclature.

(iii) The surface elevation η is assumed to be small compared to film thickness h. That is,
$\eta << h$.

(iv) The induced magnetic field is negligible compared to the applied magnetic field since the fluid considered is poorly conducting (i.e., $\sigma << 1$).

Following the above assumptions and approximations (i.e., Stokes and lubrication approximations) and also assuming that the heavy fluid in the region-2 is almost static because of creeping flow approximation in a region-2 lead the basic equations in the thin film region to the following form:

$$0 = \frac{\partial u}{\partial x} + \frac{\partial v}{\partial y} \tag{2.13}$$

$$0 = -\frac{\partial p}{\partial x} + \frac{\partial}{\partial y}\left[k_1 \left| \frac{\partial u}{\partial y} \right|^{m-1} \frac{\partial u}{\partial y} \right] + \rho_e E_x \tag{2.14}$$

$$0 = -\frac{\partial p}{\partial y} + \rho_e E_y . \tag{2.15}$$

For fully developed flow, Eq. (2.10) becomes

$$\frac{\partial^2 \phi}{\partial y^2} + \alpha \frac{\partial \phi}{\partial y} = 0 . \tag{2.16}$$

The solution of this equation using the boundary conditions (2.11) and (2.12) is

$$\phi = \frac{v_0}{h}\left[x - \frac{x_0}{1-e^{-\alpha h}}(1-e^{-\alpha y}) \right]. \tag{2.17}$$

Equations (2.4a), using Eq.(2.17), becomes

$$\rho_e = -\frac{v_0}{h}\frac{x_0 \alpha^2 e^{-\alpha y}}{1-e^{-\alpha h}} \tag{2.18}$$

and hence

$$\rho_e E_X = -\rho_e \frac{\partial \phi}{\partial x} = \frac{v_0^2}{h^2}\frac{x_0 \alpha^2 e^{-\alpha y}}{1-e^{-\alpha h}}. \tag{2.19}$$

3. DISPERSION RELATION

To find the dispersion relation, first we have to find the velocity distribution from Eq. (2.14) using the following boundary and surface conditions:

i) The no-slip condition at the rigid surface :

$$u = 0 \quad \text{at} \quad y = 0 \tag{3.1}$$

ii) The no shear condition :

$$\frac{\partial u}{\partial y} = 0 \quad \text{at} \quad y = h \tag{3.2}$$

iii) The kinematic condition :

$$v = \frac{\partial \eta}{\partial t} \quad \text{at} \quad y = h \tag{3.3}$$

iv) The dynamic condition :

$$p = -\delta\eta - \gamma \frac{\partial^2 \eta}{\partial x^2} \pm \varepsilon_e \frac{E_x^2 \eta}{h} \quad \text{at} \quad y = h. \tag{3.4}$$

where physical quantities are defined in the nomenclature.

The solution of (2.14) subject to the above conditions is

$$u = \frac{1}{k_1 b(m)}\left[\frac{\partial p}{\partial x}\frac{y^2}{2} - \frac{v_0^2}{h^2}\frac{e^{-\alpha y}}{1-e^{-\alpha h}} \right] + a_1 y + a_2 \tag{3.5}$$

where

$$a_1 = -\frac{1}{k_1 b(m)}\left[\frac{\partial p}{\partial x} + \frac{v_0^2 \alpha e^{-\alpha h}}{h^2(1-e^{-\alpha h})} \right]$$

$$a_2 = \frac{v_0^2}{k_1 b(m) h^2 (1-e^{-\alpha h})}.$$

After integrating Eq.(2.13) with respect to y between $y = 0$ and h and using Eq.(3.5), we get

$$v(h) = -\int_0^h \frac{\partial u}{\partial x} dy = \frac{h^3}{3k_1 b(m)}\frac{\partial^2 p}{\partial x^2}. \tag{3.6}$$

Equation (3.3), using (3.6) and (3.4), becomes

$$\frac{\partial \eta}{\partial t} = -\frac{h^3}{3k_1 b(m)}\left[\left(\delta \pm \frac{\varepsilon_e E_x^2}{h} \right)\frac{\partial^2 \eta}{\partial x^2} + \gamma \frac{\partial^4 \eta}{\partial x^4} \right]. \tag{3.7}$$

To investigate the growth rate, *n* of the periodic perturbation of the interface, we look for the solution of Eq. (3.7) in the form

$$\eta = \eta(y)\exp\{i\ell x + nt\} \tag{3.8}$$

where the physical quantities are defined in the nomenclature.

Substituting Eq.(3.8) into (3.7), we obtain the following dispersion relation

$$n = -\frac{h^3}{3k_1 b(m)}\left[-\left(\delta \pm \frac{\varepsilon_e v_0^{\,2}}{h^2}\right)\ell^2 + \gamma\ell^4\right]. \tag{3.9}$$

Making Eq. (3.9) dimensionless using the quantities

$$n^* = \frac{nk_1}{\sqrt{\gamma\delta}},\ h^* = \frac{h}{\sqrt{\gamma/\delta}},\ \ell^* = \ell\sqrt{\gamma/\delta},\quad v^* = \frac{v_0}{h} \tag{3.10}$$

we obtain

$$n = \frac{h^3\ell^2}{3b(m)}\left[(1\pm We) - \frac{\ell^2}{B}\right] \tag{3.11}$$

where the physical quantities are defined in the nomenclature and We is the electric parameter physically represents the measure of electric energy to pressure energy, $b(m)$ is a fitting constant and *B* is the Bond number measures the relative importance of gravitational force to surface tension. The positive or negative sign in front of *We* in the above equation will depend on whether the potential difference is along or opposing the gravity. Since the potential difference is opposing the gravity, we have chosen the negative sign and Eq. (3.11) takes the form

$$n = \frac{h^3\ell^2}{3b(m)}\left[(1-We) - \frac{\ell^2}{B}\right]. \tag{3.12}$$

This is the required dispersion relation. Thus the fitting constant *b*(*m*) should be chosen in such a way that *b*(1) =1. Thus we consider the following cases for discussion

Case (i): $b(m) = \dfrac{m+1}{2}$.

Case (ii): $b(m) = \dfrac{1}{2} + \dfrac{m}{4} + \dfrac{m^2}{4}$.

The dispersion relation (3.12) is computed for different values of *m*, *h*, We *and B* suitable for shear thinning and shear thickening flows and the results are shown in Figs.2 – 9 for the above two cases.

Setting $n = 0$ in Eq.(3.12), we obtain the cut-off wave number, ℓ_{ct} in the form

$$\ell_{ct} = \sqrt{B(1-We)}. \tag{3.13}$$

The maximum wave number, ℓ_m obtained from Eq.(3.12) by setting $\partial n/\partial\ell = 0$ is

$$\ell_m = \sqrt{\frac{B(1-We)}{2}} = \frac{\ell_{ct}}{\sqrt{2}}. \tag{3.14}$$

We note that in the case of applied voltage opposing the gravity ℓ_{ct} and ℓ_{m} are real only if $We \le 1$. However, in the case of applied voltage in the direction of gravity we get $1+We$ in Eqs. (3.13) and (3.14) and hence in that situation ℓ_{ct} and ℓ_{m} are real for all values of We.

The corresponding maximum growth rate, n_m for applied voltage opposing the gravity is

$$n_m = \frac{h^3 B}{12 b(m)} \left(1 - We\right)^2. \tag{3.15}$$

This growth rate n_m will be zero for $We = 1$. Physically this implies the equi-partition of energy (i.e., electric energy balances with pressure energy. Since pressure has the dimension of kinetic energy, this equi-partition can also be stated as electric energy balances with kinetic energy). If we choose the voltage such that $We = 1$, asymmetry can be completely reduced and hence maximum efficiency of IFE may be achieved.

Similarly, the maximum classical growth rate, n_{bm}, for $We = 0$ using $\ell_m = \sqrt{B/2}$, is given by

$$n_{bm} = \frac{B}{12} \tag{3.16}$$

Therefore,

$$G_m = \frac{n_m}{n_{bm}} = \frac{h^3}{b(m)} \left(1 - We\right)^2. \tag{3.17}$$

The growth rate given by Eq. (3.12) is also computed numerically for different values of parameters and the results are presented graphically in Figs.2-9.

For case (i): $b(m) = \dfrac{m+1}{2}$

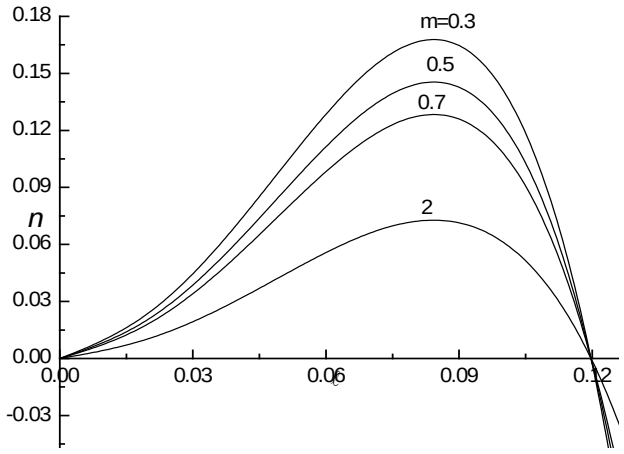

Fig. 2: Growth rate, n versus the wave number, ℓ for different values of power-law index m when $h = 5$, $B = 0.02$ and $We = 0.25$.

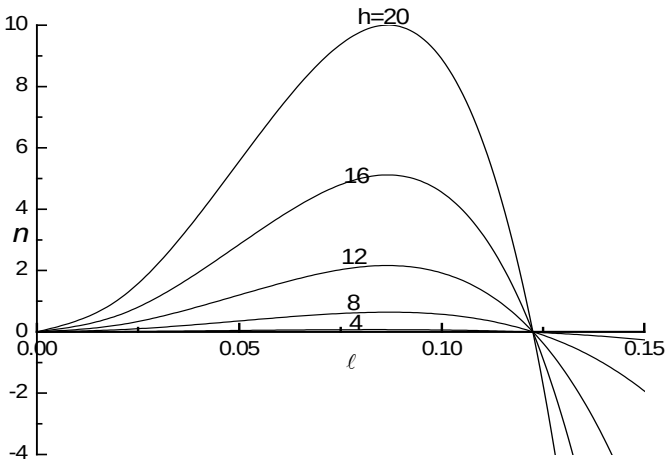

Fig. 3: Growth rate, n versus the wave number, ℓ for different values of thickness parameter h when $m = 0.5$, $B = 0.02$ and $We = 0.25$.

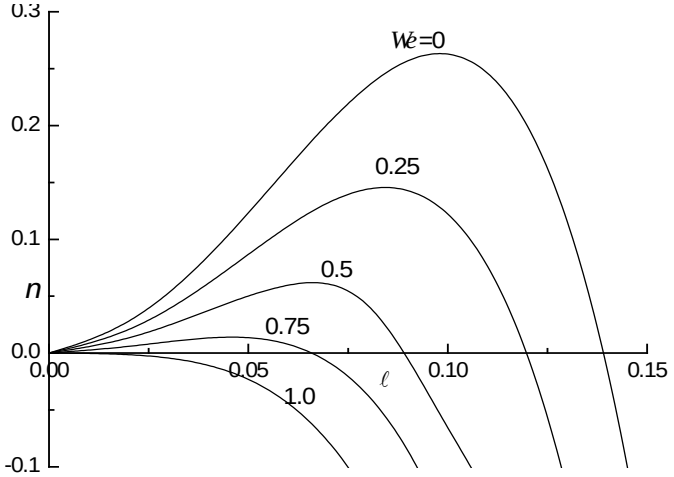

Fig. 4: Growth rate, *n* versus the wave number, ℓ for different values of electric parameter, *We* when *h = 5, m = 0.5* and *B=0.02*.

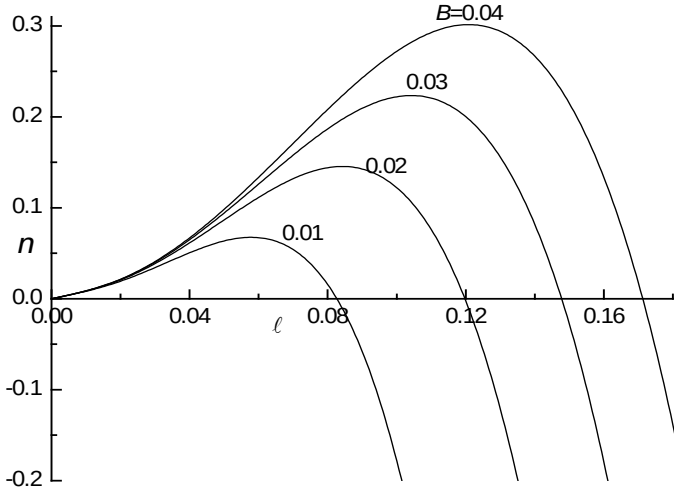

Fig. 5: Growth rate, *n* versus the wave number, ℓ for different values of Bond number, *B* when *h =5, m = 0.5* and *We = 0.25*.

For Case (ii) : $b(m) = \frac{1}{2} + \frac{m}{4} + \frac{m^2}{4}$

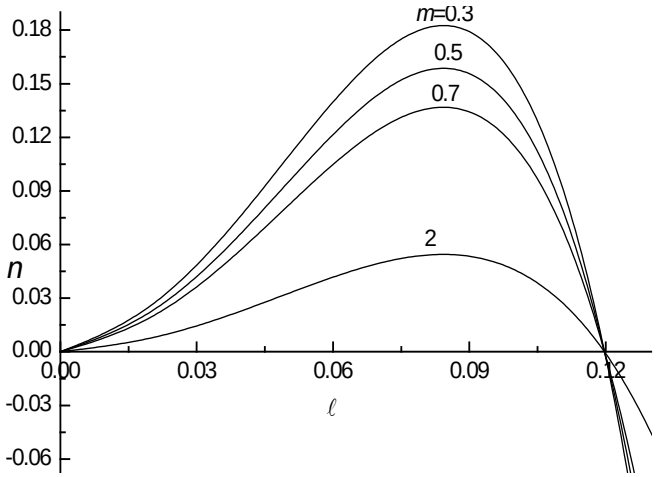

Fig. 6: Growth rate, *n* versus the wave number, ℓ for different values of power-law index *m* when *h = 5, B= 0.02* and *We = 0.25*.

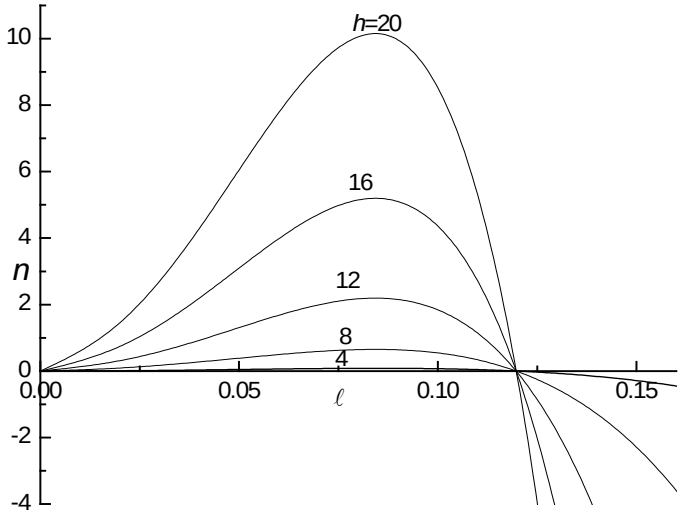

Fig. 7: Growth rate, *n* versus the wave number, ℓ for different values of thickness parameter *h* when *m= 0.5*, *B= 0.02* and *We*= 0.25.

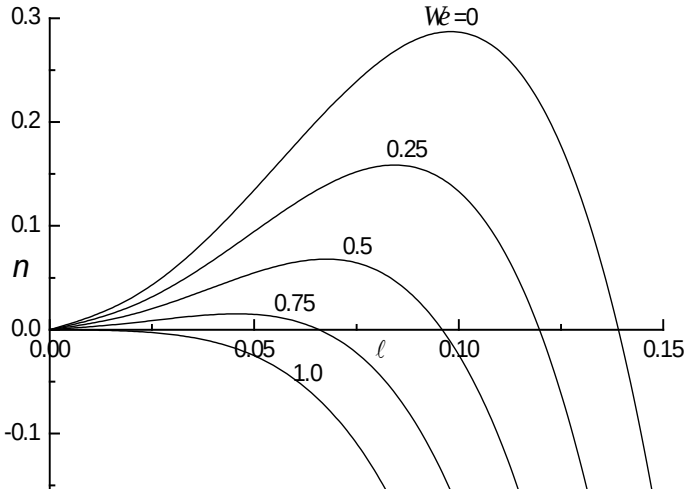

Fig. 8: Growth rate, *n* versus the wave number, ℓ for different values of electric parameter *We* when *h =5*, *m = 0.5* and *B=0.02*.

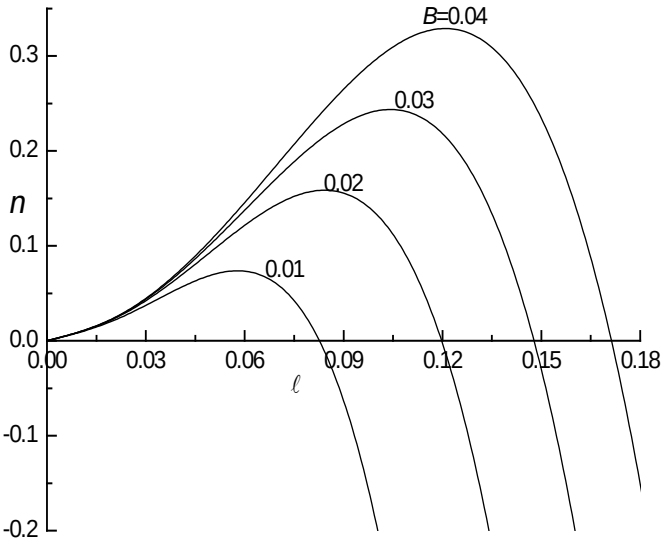

Fig. 9: Growth rate, *n* versus the wave number, ℓ for different values of Bond number *B* when *h=5*, *m = 0.5*and *We= 0.25*.

5. RESULTS AND DISCUSSION

The linear electrohydrodynamic Rayleigh-Taylor instability (ERTI) in a power-law fluid layer bounded above by a heavier fluid and below by a rigid surface in the presence of electric field is investigated**.**

Regarding the influence of power-law index *m*, it is noted that stable, marginally stable or unstable nature of the system will depend on the value of power-law index *m.* The dispersion relation is computed numerically for different values of power-law index *m*, *We*, *B*, film thickness *h*, and wave number ℓ and results are presented graphically in Figs.2-9. It is found that the nature of dispersion relation is influenced by both the reciprocal of the characteristic length δ/γ and the power-law index *m*. That is, increase in the power-law index *m* decreases the growth rate as shown in Figs.2 and 6 for both the cases of *b(m)* considered with fixed $h=5,\ B=0.02$ and $We=0.25$. The increase in the film thickness parameter *h* increases the growth rate as shown in Figs. 3 and 7 for both cases of *b(m)* with fixed $B=0.02, m=0.5 and\ We=0.25$. From Figs.4 and 8, it is clear that the decrease in growth rate compared to the classical growth rate is very steep for We in the range 0.5 to 1.0 when $B=0.02, m=0.5\ and\ h=5$. Figures 5 and 9 show the variation of the Bond number, *B* with fixed $h=5, m=0.5\ and\ We=0.25$ and found that the perturbations of the interface having ℓ smaller than the critical wave number ℓ_{ct} are amplified when δ >0 (i.e.,$\rho_f <$ ρ_h) and the growth rate decreases with decrease in *B.* Hence, the Bond number is reciprocal of surface tension and thus showing that an increase in surface tension decreases the growth rate and hence make the interface more stable.

ACKNOWLEDGEMENT

Author wish to thank Prof. Purnachandra Tejasvi, Principal, Government First Grade College, Yellapur (U.K) for their encouragement and support in doing research".

REFERENCES

1. Chandrasekhar, S., Hydrodynamic and Hydromagnetic Stability, Oxford University Press, Oxford, 1961.
2. Kull, H. J., Theory of Rayleigh-Taylor Instability, Phys. Report, 1991, 206, 198.
3. Rudraiah, N., Krishnamurthy, B. S. and Mathad, R. D., The Effect of Oblique Magnetic Field on the Surface Instability of a Finite Conducting Fluid Layer, Acta, Mech., 1996, 119, 165.
4. Babchin, A. J., Frenkel, A. L., Levich, B. G., Shivashinsky, G. I., Nonlinear Saturation of Rayleigh-Taylor Instability in Thin Films, Phys. Fluids, 1983, 26, 3159.
5. Rudraiah N, Wagner C, Evans G. S. and Friedrich R., Nonlinear study of Rayleigh-Taylor instability in thin films past a porous layer, Indian J. Pure Appl. Math., 1998, 29(4), 417.
6. Brown, H. C., Rayleigh-Taylor instability in a finite thickness layer of a viscous fluid, Phys. Fluid A, 1989,1(5), 895.
7. Rudraiah, N., and Kaloni, P. N., Flow of non-Newtonian fluids, Encyclopaedia of Fluid Mechanics, Gulf publishing company, USA. 1990, Chapter 1, 9, 1.
8. Sharp, D. H., An over view of Rayleigh-Taylor instability, Physica D, 1984, 12, 3.
9. Ng, C. O., Rudraiah, N., Nagaraj, C., Nagaraj, H. N., Electrohydrodynamic Dispersion of Macromolecular Components in nanostructured biological bearing, J. of Energy, Heat Mass Transfer, 2005, 27, 39.
10. Rudraiah N, K. B. Chavaraddi, I.S. Shivakumara and B. M. Shankar., Electrohydrodynamic Rayleigh-Taylor instability in a non-Newtonian fluid layer bounded above by a porous layer, International Journal of Applied Mathematics & Engineering Sciences, Vol. 5, No. 1, January-June 2011, 45.

NOMENCLATURE

B	Bond number ($\delta\lambda^2/\gamma$)
$b(m)$	fitting constant
C	concentration
C_0	reference concentration
$\vec{g}$	gravitational acceleration
h	fluid film thickness
H	thickness of porous layer
$\vec{J}$	current density
k_1	consistency index
ℓ	wave number
m	index parameter

n	growth rate
P	pressure
$\vec{q}$	velocity
S	Strouhal number ((L/TU)
U	characteristic velocity
T	characteristic time($\mu\gamma / h^3\delta^2$)
We	electric parameter($\varepsilon_e v_0^{\,2} / \delta h^3$)
$x,y,$	coordinates
u,v	velocity coordinates

GREEK SYMBOLS

α_h	volumetric expansion coefficient of σ
δ	drag constant
ε_e	dielectric constant
ρ	fluid density
ρ_e	density of charges
σ	electrical conductivity
μ	fluid viscosity
$\vec{\tau}_i$	stress tensor
ϕ	electric potential
∇	differential operator
ν	kinematic viscosity (μ / ρ)
γ	surface tension

Source of support: Department of Collegiate Education, Government of Karnataka, India.
Conflict of interest: None Declared

